Video Article

In Vitro Reconstitution of Self-Organizing Protein Patterns on Supported Lipid Bilayers

Beatrice Ramm*[1], Philipp Glock*[1], Petra Schwille[1]

[1]Department of Cellular and Molecular Biophysics, Max Planck Institute of Biochemistry

*These authors contributed equally

Correspondence to: Petra Schwille at schwille@biochem.mpg.de

URL: https://www.jove.com/video/58139
DOI: doi:10.3791/58139

Keywords: Biochemistry, Issue 137, In vitro reconstitution, MinD, MinE, supported lipid bilayer, pattern formation, microstructures, self-organization

Date Published: 7/28/2018

Citation: Ramm, B., Glock, P., Schwille, P. *In Vitro* Reconstitution of Self-Organizing Protein Patterns on Supported Lipid Bilayers. *J. Vis. Exp.* (137), e58139, doi:10.3791/58139 (2018).

Abstract

Many aspects of the fundamental spatiotemporal organization of cells are governed by reaction-diffusion type systems. *In vitro* reconstitution of such systems allows for detailed studies of their underlying mechanisms which would not be feasible *in vivo*. Here, we provide a protocol for the *in vitro* reconstitution of the MinCDE system of *Escherichia coli*, which positions the cell division septum in the cell middle. The assay is designed to supply only the components necessary for self-organization, namely a membrane, the two proteins MinD and MinE and energy in the form of ATP. We therefore fabricate an open reaction chamber on a coverslip, on which a supported lipid bilayer is formed. The open design of the chamber allows for optimal preparation of the lipid bilayer and controlled manipulation of the bulk content. The two proteins, MinD and MinE, as well as ATP, are then added into the bulk volume above the membrane. Imaging is possible by many optical microscopies, as the design supports confocal, wide-field and TIRF microscopy alike. In a variation of the protocol, the lipid bilayer is formed on a patterned support, on cell-shaped PDMS microstructures, instead of glass. Lowering the bulk solution to the rim of these compartments encloses the reaction in a smaller compartment and provides boundaries that allow mimicking of *in vivo* oscillatory behavior. Taken together, we describe protocols to reconstitute the MinCDE system both with and without spatial confinement, allowing researchers to precisely control all aspects influencing pattern formation, such as concentration ranges and addition of other factors or proteins, and to systematically increase system complexity in a relatively simple experimental setup.

Video Link

The video component of this article can be found at https://www.jove.com/video/58139/

Introduction

Spatiotemporal patterns are essential in nature, regulating complex tasks both on the multicellular and cellular level, from morphogenesis to regulated cell division[1,2]. Reaction-diffusion systems play an important role in establishing these patterns, but are still not well understood. A prime example of a reaction-diffusion system and the best characterized biological system so far is the *Escherichia coli* MinCDE system[3,4,5,6,7]. The MinCDE system oscillates from cell pole to cell pole in *E. coli* to determine the middle of the cell as the future division site. This system is based on the ATPase MinD, the ATPase activating protein MinE, and the membrane as a spatial reaction matrix[8]. MinC is not part of the pattern formation mechanism, but is the actual functional agent: an inhibitor of the main divisome protein FtsZ[5,6]. MinC binds to MinD and therefore follows the oscillations, resulting in a time-averaged protein concentration gradient that is maximal at the cell poles and minimal at the cell middle, only allowing FtsZ to polymerize at midcell[9,10]. The MinCDE system is part of the larger family of Walker A ATPases that are key to the spatiotemporal organization in bacteria[2], for positioning and transporting protein complexes[11] and plasmids[12] and for regulating cell division[13] and chromosome segregation[14]. Hence, the MinCDE reaction-diffusion system not only represents an archetypal reaction-diffusion system, but has also attracted attention because of its relevance for the spatiotemporal organization in bacteria.

Detailed functional studies of the MinCDE system *in vivo* are complicated, as manipulation of proteins and gene deletion typically result in cell division defects. Furthermore, changing the membrane composition or the properties of the cytosol *in vivo* is very challenging[15,16]. Changes to the system and influencing factors are hard to interpret in the complex environment of the cell, even more so if it is disturbed in such an essential function as cell division. We and others have therefore turned to an *in vitro* reconstitution approach, reducing the system to its core components: MinD, MinE, ATP as an energy source, and the supported lipid bilayer as a reaction matrix[6,17,18]. This bottom-up approach allows to probe the mechanism of self-organization in detail without the complexity of a living cell. The proteins form traveling surface waves[6] and other kinds of patterns[17,19] under these conditions, albeit with a wavelength that is usually about a magnitude larger than *in vivo*. The use of an open chamber facilitates precise control over all aspects influencing pattern formation: protein concentrations[6], protein properties[20], membrane composition[10], buffer composition, and ATP concentration[6], as well as addition of other factors such as crowding agents[21] and other divisome proteins[22]. In comparison, the *in vitro* reconstitution of the MinCDE system in a flow-cell[18,19,23] can be used to probe the influence of flow[17,23], protein limiting conditions[19], membrane composition[19] and full 3D confinement[18] on protein patterns, but renders an exact control of protein/component concentration and sequential component addition much more complicated.

Using this open chamber, we also patterned the support of the planar lipid bilayers by which one can probe how geometrical boundaries influence pattern formation[21], a phenomenon that has recently also been investigated *in vivo* using bacteria molded into microstructures[7]. We also employed this assay to investigate how defined mutations in MinE affect pattern formation of the system[20]. Furthermore, the same basic assay format has been employed to investigate how pattern formation can be controlled by light, introducing an azobenzene-crosslinked MinE peptide into the assay, and imaging with TIRF microscopy[24].

We found that, in order to replicate the MinDE pattern formation observed *in vivo* in an *in vitro* system, confinement was key. Using rod-shaped microcompartments, with dimensions adjusted to the larger wavelength of MinDE *in vitro* (10 x 30 µm), clad with a supported lipid bilayer allowed the reconstitution of MinDE pole-to-pole oscillations and protein gradient formation[10,25]. In this assay, the supported lipid bilayers are deposited on a patterned PDMS substrate that contains several hundred replicas of rod-shaped microcompartments that remain open on the top. By this, the reaction can be set up in an open chamber, and subsequently the buffer is lowered to the rim of the microcompartments, thereby confining the reaction to a small volume. Even though these compartments have an air-buffer interface on one side and hence do not represent a full 3D confinement by membrane, the protein dynamics mimicked *in vivo* oscillations[10,25]. Compared to full 3D confinement, which shows very similar results[18], the open microstructures assay is relatively simple and easy to handle and can also be performed by laboratories that are not equipped with specialized microfluidics equipment and clean-room facilities.

Here, we present an experimental protocol for reconstituting MinCDE pattern formation on supported lipid bilayers *in vitro* using an open chamber that allows for control of all components and easy access by optical microscopy and, with minor modifications, is also adaptable for surface-probe techniques[26]. Next to planar supported lipid bilayers, we also show how protein confinement can be obtained using simple patterned supported lipid bilayers on rod-shaped PDMS microstructures. These assays, although optimized for the MinCDE system, can also be transferred to other protein systems that interact in a similar way with the membrane, such as FtsZ[27] or a minimal actin cortex[28].

Protocol

1. Protein Production

1. Protein expression
    1. Transform *E. coli* BL21 (DE3) pLysS with the respective plasmid for expression of MinD[6], EGFP-MinD[29], mRuby3-MinD[24], MinE[6] or MinC[30]. For plasmid maps, please see supplementary information.
    2. Inoculate an overnight culture in LB medium with a single colony using the respective antibiotics (*e.g.,*100 µg/mL Ampicillin or 50 µg/mL Kanamycin) and incubate at 37 °C for 14-16 h while shaking.
    3. Inoculate 500 mL of TB medium containing the respective antibiotic with the overnight culture (1:200 dilution) and incubate culture at 37 °C while shaking at 180 rpm.
    4. Induce protein expression by adding 0.5 mM IPTG when the culture reaches an optical density at 600 nm of 0.5-0.7. In case of EGFP-MinD or mRuby3-MinD, shift cells to an incubator with 16 °C and grow cells for 14-16 h, and in case of MinC, MinD or MinE, grow cells for 3-4 h at 37 °C after induction.
    Note: Induction of MinC, MinD or MinE expression is toxic for the cells, as overexpression results in cell division defects; hence, it is important that incubation time at 37 °C is kept below 4 h. If more protein is needed, increase the amount of culture, but not incubation time.
    5. After respective incubation time harvest cells by centrifugation at 4000 x g for 10 min and store the cell pellet at -80 °C until further use.

2. Protein purification
Note: Proteins can be purified either using prepacked Ni-NTA columns on an automated protein purification system or using Ni-NTA beads for gravity-flow bench purification.
    1. For purification with prepacked Ni-NTA columns on automated protein purification systems use buffer A1 (50 mM sodium phosphate pH 8.0, 500 mM NaCl, 10 mM imidazole), buffer B1 (50 mM sodium phosphate pH 8.0, 500 mM NaCl, 20 mM imidazole), and buffer C1 (50 mM sodium phosphate pH 8.0, 500 mM NaCl, 250 mM imidazole). For gravity-flow bench purification using Ni-NTA beads use buffer A2 (50 mM Tris-HCl pH 8.0, 300 mM NaCl, 10 mM imidazole), buffer B2 (50 mM Tris-HCl pH 8.0, 300 mM NaCl, 20 mM imidazole), and buffer C2 (50 mM Tris-HCl pH 8.0, 300 mM NaCl, 250 mM imidazole). Supplement all buffers with 10 mM ß-mercaptoethanol or 0.4 mM TCEP (tris(2-carboxyethyl)phosphine) as reducing agent right before use.
    2. Resuspend cells in 20-30 mL of buffer A1 or A2 supplemented with EDTA-free protease inhibitor, 100 µg/mL lysozyme, ~250 U/mL DNase and 0.2 mM Mg^{2+}-ADP (Mg^{2+}-ADP in case of MinD or EGFP-MinD purification only, from a 100 mM ADP stock in 100 mM $MgCl_2$ with pH adjusted to 7.5).
    3. Lyse cells using a tip sonicator (30% amplitude, 2.5 min, 30 s pulse, 30 s off) while keeping the vial containing the cells in an ice bath.
    4. Remove cell debris by centrifuging the cell lysate for 45 min at 25,000 x g and 4 °C.
    5. Incubate the supernatant on Ni-NTA column or Ni-NTA beads.
        1. For prepacked Ni-NTA columns, load the sample onto the column using the sample pump of an automated protein purification system.
        2. For bench-top purification, incubate the sample with Ni-NTA beads in a 50 mL reaction tube on a rotating shaker at 4 °C for 1 h. For the subsequent steps, transfer the Ni-NTA beads into an empty column using a 25 mL pipette.
    6. Wash with at least 5 column volumes of buffer A1 or A2.
    7. Wash with at least 5 column volumes of buffer B1 or B2.
    8. Elute protein with buffer C1 or C2.
    9. Assess protein purity via SDS-PAGE.
    10. Optional: Further purify protein by applying it to a gel filtration column equilibrated in storage buffer (50 mM HEPES/KOH pH 7.2, 150 mM KCl, 10% glycerol, 0.1 mM EDTA, 0.4 mM TCEP, (0.2 mM Mg^{2+}-ADP in case of MinD)).
    Note: Gel filtration is recommended for MinD to remove aggregated protein fraction.

11. If no gel-filtration is employed, exchange Ni-NTA elution buffer to storage buffer (50 mM HEPES/KOH pH 7.2, 150 mM KCl, 10% glycerol, 0.1 mM EDTA, 0.4 mM TCEP, (0.2 mM Mg-ADP in case of MinD)) using a gravity flow desalting column (see **Table of Materials**).
12. Shock-freeze proteins in aliquots in liquid nitrogen and store at -80 °C until further use.
13. Measure protein stock concentration using Bradford Assay, and determine protein activity with an ATPase assay[20].
    Note: Do not assess protein concentration using absorption at 280 nm. The presence of nucleotide during MinD purification and the lack of tryptophans in MinE distort A_{280} concentration measurements. Use Bradford or BCA assays to measure protein concentrations instead.

3. Protein labeling
   Note: The fusion of a fluorescent protein to the small protein MinE induces major changes to its diffusive properties and function; hence, chemical labeling of the protein (cysteine at position 51) is preferred over fusion to fluorescent proteins.
   1. Dissolve 0.125 mg of maleimide-dye conjugate in 5-10 µL of DMSO (dimethyl sulfoxide) and add under shaking to a 0.5 mL MinE aliquot in storage buffer at pH 7.2, prepared as detailed above.
   2. Incubate for 2 h to overnight at 4 °C or 2 h at RT under gentle shaking or stirring.
   3. Separate dye and protein using a gravity flow desalting column equilibrated with storage buffer (50 mM HEPES/KOH pH 7.2, 150 mM KCl, 10% glycerol, 0.1 mM EDTA, 0.4 mM TCEP).
   4. To further remove any unattached dye, dialyze the protein against an excess of storage buffer.
   5. Verify successful labelling by measuring the extinction at the maximum for the respective dye and calculate the estimated labeling efficiency. Please refer to the dye manufacturer's instructions for a detailed protocol on estimating the degree of labeling. Analyze with SDS-PAGE and determine total mass by mass spectrometry for further useful information about sample homogeneity and labeling success.

2. Small Unilamellar Vesicle (SUV) Preparation

1. Generation of multilamellar vesicles
   1. Calculate the amount of lipid(s) in chloroform for your desired mixture and final SUV volume. The concentration should be 4 mg/mL of lipids in Min buffer (25 mM Tris-HCl pH 7.5, 150 mM KCl, 5 mM $MgCl_2$). For a standard Min assay a mixture of 7:3 DOPC:DOPG (mol percent) is recommended. When using *E. coli* polar lipid extract, use SLB buffer (25 mM Tris-HCl pH 7.5, 150 mM KCl) for all preparation steps.
      Note: It is not recommended for first time users to use *E. coli* polar lipid extract as the generation of homogenous SLBs with this mixture is much more challenging.
   2. Using a positive displacement pipette with glass tips, mix the lipids in chloroform in a 1.5 mL glass vial.
      1. Dry the lipids under a slight nitrogen stream while slowly turning the vial. Place the lipids under a stronger nitrogen stream for 10 to 20 minutes. Place the vial containing the dried lipid film in a vacuum desiccator and apply vacuum for at least 1 h.
   3. Rehydrate the lipids in Min buffer by vortexing at room temperature until the mixture is homogeneously opaque.
      Note: For generation of small unilamellar vesicles from multilamellar vesicles, lipids can either be extruded as described in 2.2. or sonicated as described in 2.3. In general, extrusion yields a narrower size distribution which can help with formation of supported lipid bilayers.

2. SUV preparation by extrusion
   1. Break lipid aggregates and multilamellar structures and further solubilize lipids by freeze-thawing for 7 to 10 cycles.
      1. Prepare a beaker with water at 70° C to 99° C on a hot plate and a container with liquid nitrogen.
      2. Hold the vial in liquid nitrogen with large tweezers until the nitrogen stops boiling. Then transfer the vial to hot water until the solution is completely thawed. Repeat these steps until the lipid mixture appears clear to the eye, depending on the mixture.
   2. Assemble a lipid extruder and pre-rinse the system with Min buffer. Extrude the lipid mixture between 35 and 41 times through a membrane of 50 nm pore size. Make sure to end on an odd number of passes to avoid aggregates that never traversed the membrane.

3. SUV preparation by sonication
   1. To better dissolve lipids in the buffer, put the glass vial containing the solution in a heat block set to 37 °C and vortex every 20 minutes for 1 minute. Incubate in total for about 1 h.
   2. Immerse the bottom of the vial in a sonicator bath (in this work 1.91 L, 80 W) by attaching the vial onto a clamp stand at the required height.
   3. Set the water height in the sonicator bath so that the solution surrounding the vial is thoroughly agitated by the pulses and sonicate the lipid mixture for about 20 minutes. Check for successful sonication by assessing the clarity of lipids.

4. SUVs can be stored at 4 °C for up to a week or frozen at -20 °C in small aliquots (~20 µL) and stored for several weeks. Thaw vials or tubes at room temperature and sonicate again as described under 2.2.3 or 5.3 until the solution is clear before using SUVs for preparation of supported lipid bilayers (SLBs). Please note that the narrow size distribution of SUVs obtained by extrusion is lost after freezing and subsequent thawing and sonication.

3. Cleaning Glass Coverslips

Note: Cleaning and hydrophilization of glass coverslips is an important factor for homogenous and fluid supported lipid bilayers. Glass coverslips can be cleaned using a piranha solution, made from a ratio of 7:2 sulfuric acid to 50% hydrogen peroxide (3.1), or with an oxygen plasma in a plasma cleaner (3.2). Both methods yield similar results.

1. Piranha cleaning of coverslips
    1. Apply piranha solution
        1. Distribute glass coverslips on an inverted glass Petri dish or other inert surface. With a glass pipette, add 7 drops of concentrated sulfuric acid (98%) to the center of each coverslip.
        CAUTION: Sulfuric acid is strongly acidic and corrosive. Work in a fume cupboard and with proper protective equipment only.
        2. Add two drops of 50% hydrogen peroxide to the middle of the acid drops.
        CAUTION: Hydrogen peroxide is corrosive to the eyes and skin.
        3. Cover the reaction and incubate for at least 45 minutes.
        Note: The maximum waiting time here is not critical for the outcome of the experiment and can be extended up to several days.
    2. Wash piranha cleaned coverslips.
        1. Pick up the coverslips individually using tweezers and rinse off acid with ultrapure water. Place the washed coverslips in non-stick holders or similar transportation device.
        2. Rinse each coverslip extensively with ultrapure water and dry the surface with pressurized gas (nitrogen, air only if oil-free). Mark the cleaned side of the coverslip with permanent marker.

2. Plasma cleaning of coverslips
    1. Rinse coverslips with excess ethanol and afterwards with excess ultrapure water. Dry coverslips with pressurized gas. Assemble chamber as described in 4.
    2. After chamber assembly as described in 4 take the coverslips with attached chamber and place in plasma cleaner with oxygen as process gas. Clean coverslips with plasma (in this work 30% power, 0.3 mbar oxygen pressure for 1 min was used). Do the cleaning right before SLB formation as described in 5, as the hydrophilizing effect of plasma cleaning wears off over time.
    Note: Timing and power of plasma cleaning should be optimized using fluorescently labeled membranes, as too little or excessive plasma cleaning can both lead to immobile membranes or membranes with holes.

4. Chamber Assembly

1. With sharp scissors, cut off and discard the lid and the conical part of a 0.5 mL reaction tube. Apply UV-glue to the upper rim of the tube and distribute evenly by using a pipette tip.
2. Glue the tube upside down to the previously cleaned coverslip. In case of piranha cleaning make sure to glue it to the cleaned side of the glass. Cure the UV-glue by placing multiple chambers underneath a 360 nm lamp or LED for 5 to 15 minutes.

5. Supported Lipid Bilayer (SLB) Formation

1. Pre-heat heat block to 37 °C and incubate 2 mL reaction tubes with Min or SLB buffer, 1 tube per chamber.
2. Blow nitrogen into the assembled and cured chambers to remove any dust or other particles that may have settled during the UV curing and assembly. Plasma clean as described in 3.2 if you have not cleaned your coverslips with Piranha solution (3.1). Place chambers on heat block.
3. Dilute a 20 µL aliquot of clear lipids (at 4 mg/mL) with 130 µL of Min buffer or SLB buffer in case of *E. coli* polar lipid extract, yielding a working concentration of 0.53 mg/mL. In case lipids were frozen, sonicate first by holding the tube into a bath sonicator before adding buffer, then sonicate again with buffer.
4. Add 75 µL of lipid mixture to each chamber and set a timer to 3 minutes (for DOPC/DOPG mixtures; longer incubation may be necessary for other lipid mixtures). In case of *E. coli* polar lipid extract, pipette $CaCl_2$ from a 100 mM stock into the chamber to a final concentration of 3 mM. During the incubation time, the vesicles burst on the hydrophilic glass surface and fuse to form a coherent SLB.
5. After 60 seconds, add 150 µL of Min buffer to each chamber.
6. Washing the chambers: After another 120 seconds (3 minutes total) wash each chamber by adding 200 µL of Min or SLB buffer, carefully pipetting up and down a few times, removing and adding another 200 µL.
    1. After each chamber has been washed once, proceed to wash the first chamber thoroughly until the 2 mL of buffer are used up. Washing of SLBs needs some experience to perfect the extent of motions in the chamber and find the correct washing intensity.
    Note: Never remove all liquid from the chamber to avoid drying of the SLB.
    Note: On top of washing, membrane properties will vary depending on many additional factors: Type of lipids and their relative concentrations in lipid mixtures, preparation method for SUVs, surface treatment and prior cleaning of support.

6. Self-organization Assay

1. Adjust buffer volume in the chamber to 200 µL Min buffer minus the amount of protein and ATP solution, then add MinD, labeled MinD, MinE, and, if desired, MinC. Gently mix components by pipetting. Example concentrations are 1 µM MinD (doped with 30% EGFP-MinD), 1 µM MinE (doped with 10% chemically labeled MinE) and 0.05 µM MinC, but patterns form over a range of concentrations[6,10,20,30].
2. Add 2.5 mM ATP (from 100 mM ATP stock in 100 mM $MgCl_2$, pH 7.5) to start the self-organization of MinDE.
Note: The order of the component addition (MinD, MinE and ATP) can be varied and will not influence the final pattern outcome[4].
3. Observe MinDE self-organization on the fluorescence microscope (see **Table of Materials**). MinDE self-organization can also be observed using TIRF microscopy. For imaging eGFP-MinD, use a 488 nm Argon laser or comparable diode laser (*e.g.,* 490 nm). For imaging mRuby3-MinD, it is best to employ a 561 nm diode laser.
Note: Avoid high levels of excitation for longer times as we and others[17] have observed phototoxicity in the MinDE system, leading to irreversible protein polymerization on the membrane.

7. PDMS microstructures

Note: PDMS (polydimethylsiloxane) is a polymer that can be used for the production of microstructures and microfluidic devices. A patterned silicon wafer serves as a mold for casting the PDMS structures. The PDMS structures then serve as a support for SLB formation and assay setup.

1. Either produce silicon wafer with microcompartments yourself using photolithography (see Zieske and Schwille for a detailed protocol[31] or Gruenberger *et al.* for a video protocol[32]) or order your desired silicon wafer from a foundry. For the pattern of the wafer used herein please see supplementary information.
2. Production of PDMS microstructures from patterned silicon wafers.
    1. Use a plastic cup to weigh 10 g of PDMS base and 1 g of PDMS crosslinker. Either use a mixing device to mix and degas the PDMS mixture or manually mix the PDMS and then degas under vacuum.
    2. Use a pipette tip to drop a small amount of PDMS directly onto the structure on the silicon wafer.
    Note: Be careful not to scratch the silicon wafer.
    3. Immediately place a #1 coverslip onto the PDMS drop and take the upper end of a clean pipette tip to gently press the coverslip onto the silicon wafer. The PDMS should be spreading thinly between the coverslip and the silicon wafer.
    4. Place the wafer with the coverslips into an oven and cure the PDMS for 3-4 hours or overnight at 75 °C. Remove the wafer from the oven and let it cool down to room temperature. With a razor blade, carefully remove the coverslip with the attached PDMS from SI wafer.
    Note: To prevent the silicon wafer from getting dirty or damaged, always cover the microstructures with PDMS and a coverslip. However, PDMS ages, resulting in cracks in the microstructures, hence do not use PDMS structures that are older than two to three weeks.

8. Self-organization in PDMS Microstructures

1. Use coverslips with PDMS microstructures to attach a chamber as described under 4.
2. Clean and hydrophilize surface in an oxygen plasma cleaner as described under 3.2.2. Do not piranha clean PDMS substrates.
3. Setup a MinDE self-organization assay as described under 6.
4. After setting up the assay, check for regular MinDE pattern formation and properly formed microstructures on the fluorescence microscope.
5. When regular MinDE patterns have formed (10 - 30 min), gently pipette up and down twice to mix components and then remove the buffer step by step by pipetting. Remove the large bulk of buffer using a 100 µL pipette and then carefully remove the rest using a 10 µL pipette.
Note: This step might need some practice. If too much buffer is taken out or the process takes too long, the microstructures will be dried out; if too little is taken, the proteins will not be confined in the microstructures, but continue to form traveling surface waves.
6. Immediately close the chamber with a lid to avoid drying of the residual buffer in the microstructures.
7. To allow for longer imaging times, plug a moistened piece of sponge inside the chamber and then close with lid. Make sure the sponge does not contact the surface of the coverslip.
8. Before imaging of the microstructures check on the surface that the buffer was lowered enough, so that in the surface above the microstructures MinDE pattern formation has halted. Image MinDE oscillations in microstructures. Check that microstructures are not dried out or are drying out during imaging.
Note: Discard coverslips with microcompartments after each use, as cracks in the PDMS form.

9. Analysis of MinDE pattern formation

1. Quantify wave length, wave velocity and wave profiles of the MinDE self-organization on planar supported lipid bilayers. FIJI with the standard set of packaged plugins is sufficient for basic analysis[33].
2. Analyze pole-to-pole oscillations in microcompartments by obtaining kymographs and time-averaged protein concentration profiles. Basic kymographs can be obtained by re-slicing a time series along a line selection in FIJI.

Representative Results

Protein purification following our protocol should yield Min proteins of adequate purity. As a reference, **Figure 1** provides an SDS-PAGE image of MinD, fluorescently labelled MinD, MinE, and MinC. The individual steps of the procedure to perform a MinDE self-organization assay on non-patterned supported lipid bilayers are described in **Figure 2**. Using this protocol, regular MinDE traveling surface waves can be observed throughout the chamber (**Figure 3**). The wavelength can vary slightly within the chamber, but in general patterns look similar. The edges of the chamber should not be used for quantitative comparisons, as membranes that form on the UV glue seem to have different properties than on the glass surface (see **Figure 3C**). The traveling surface waves can be analyzed by plotting the intensity along the propagation direction (**Figure 3B**). While MinD fluorescence plateaus rather fast from the leading edge of the wave and then sharply decreases at the trailing edge, MinE fluorescence increases almost linearly from the start of the MinD wave and reaches its maximum after MinD at the trailing edge, where it falls off markedly[6].

Next to protein quality, the quality of the supported lipid bilayers is most critical for a regular self-organization of MinCDE. On the one hand if the membrane is washed too excessively or the underlying surface has been cleaned and thus charged too strongly, holes can form in the membrane (**Figure 6A**, top). On the other hand if the membrane is not washed properly or the underlying surface is not cleaned/hydrophilized, vesicles will stick to the membrane or the membrane fluidity will be compromised (**Figure 6A**, bottom). Even though not as apparent as when observing the membrane directly via labeled lipids, these problems can also be detected from the MinD fluorescence signal, as patterns are not regular and the fluorescence in the maxima is not homogenous but contains "holes" or bright spots as shown in the middle panel of **Figure 6A**.

For the MinDE self-organization in rod-shaped PDMS microstructures the procedure is summarized in **Figure 4**. Several protocol steps do not need to be repeated, as proteins and lipids can be reused. Like on non-patterned substrates, the substrate is cleaned and hydrophilized (by plasma-cleaning), a supported lipid bilayer is formed on the PDMS and the self-organization assay is set up in a volume of 200 µL. To check that a proper membrane has formed and MinDE self-organizes on the membrane, the chambers are imaged. When a proper membrane has been formed, MinDE forms regular traveling surface waves on the surface of the PDMS between the individual microstructures and also self-organizes at the bottom of the microstructures as the waves can freely move over the entire membrane-covered surface (**Figure 5A**). After buffer removal, the surface between the compartments should not show any propagating MinDE patterns (**Figure 5B**), as it should be entirely dry. If MinDE patterns are still moving, more buffer needs to be removed. The proteins are now confined in the rod-shaped microcompartments by the membrane-clad PDMS and by air on the upper interface (**Figure 5C**), in which they will self-organize. Under these conditions the two proteins can perform pole-to-pole oscillations as shown in **Figure 5D**. As a fraction of MinD and MinE is always membrane-bound, also during buffer removal, the concentrations after buffer removal are not comparable to input concentrations. Due to this effect the concentrations also vary between individual microstructures on the same coverslip as they depend on the position of the patterns before buffer removal. Silicon wafer production or PDMS molding from the silicon wafer can result in incomplete microstructures that cannot be used for analysis (**Figure 6B**). Furthermore, due to the buffer removal microstructures might dry out during the process, and hence, should be excluded from further analysis (**Figure 6B**). As a result only a fraction of the microstructures in one chamber shows the desired pole-to-pole oscillations. To analyze protein dynamics in the microstructures, a kymograph can be obtained by drawing a selection over the entire structure (**Figure 5E**). When MinCDE oscillate from pole-to-pole, MinC and MinD will show a time-averaged concentration gradient with maximum concentration at the compartment poles and minimal concentration in the middle of the compartment (**Figure 5F**).

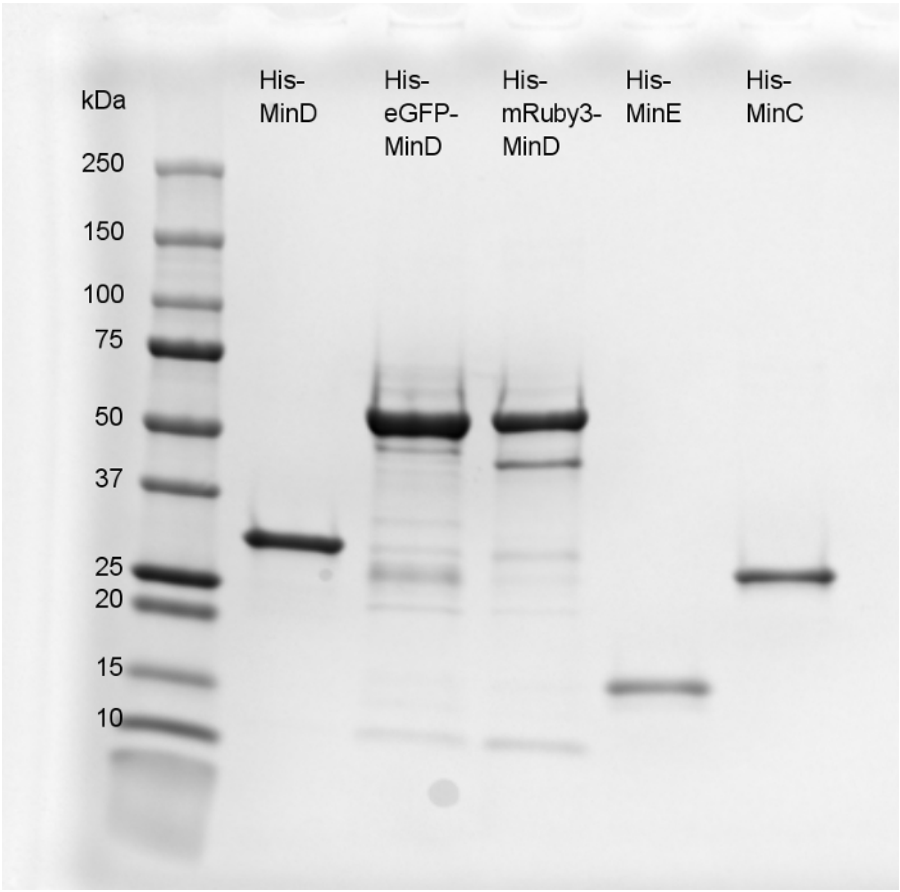

Figure 1: SDS-PAGE showing the final products of protein purifications. His-MinD (33.3 kDa), His-eGFP-MinD (60.1 kDa), His-mRuby3-MinD (59.9 kDa), His-MinE (13.9 kDa) and His-MinC (28.3 kDa) are shown in order. Please click here to view a larger version of this figure.

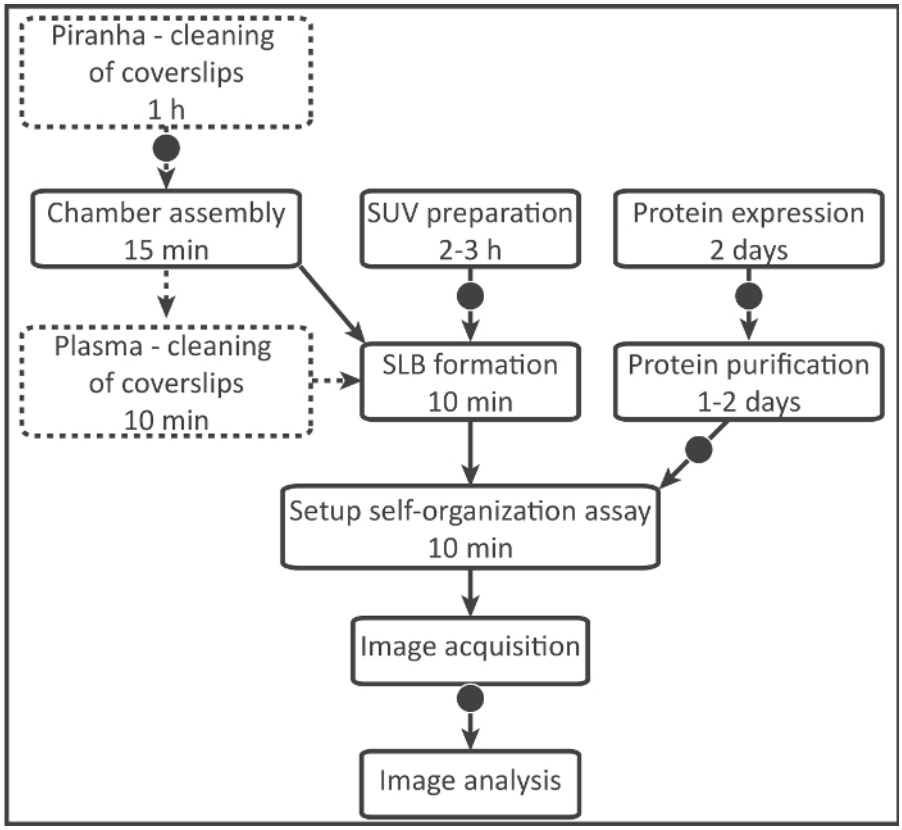

Figure 2: Process flow diagram showing the individual steps and timing of the protocol for a self-organization on non-patterned supported lipid bilayers (Steps 1-6). Dashed boxes indicate that one of these two options can be used for cleaning. Arrows marked by circles indicate where the protocol can be paused and resumed later. Please click here to view a larger version of this figure.

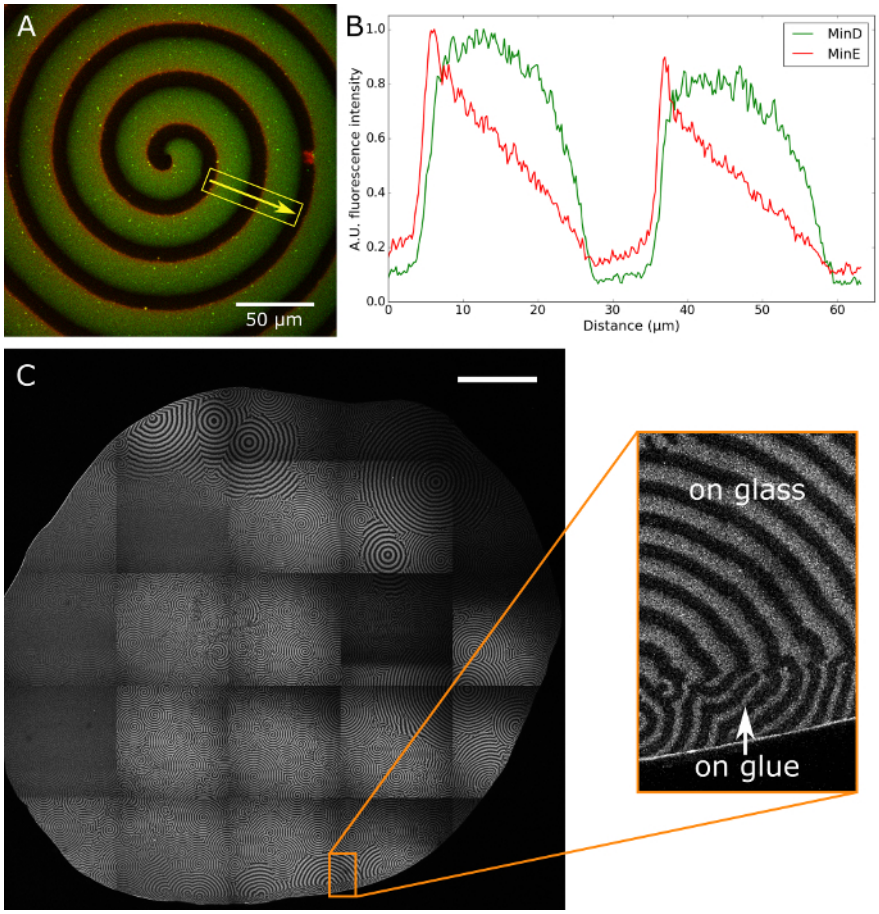

Figure 3: Imaging of MinDE assay by confocal microscopy. A) Regular Min spiral, from which wave propagation speed, intensity plot and speed measurements can be obtained. Concentrations used: 0.6 µM MinD (30% eGFP-MinD), 1.8 µM His-MinE (30% His-MinE-Alexa647) **B)** Example normalized intensity plot for the region marked in A. **C)** Overview of entire assay chamber (scale bar: 1 mm, same protein concentrations as above). Spirals turning either direction as well as target patterns can be observed. The magnified region shows how wave patterns differ on the UV-glue. Please click here to view a larger version of this figure.

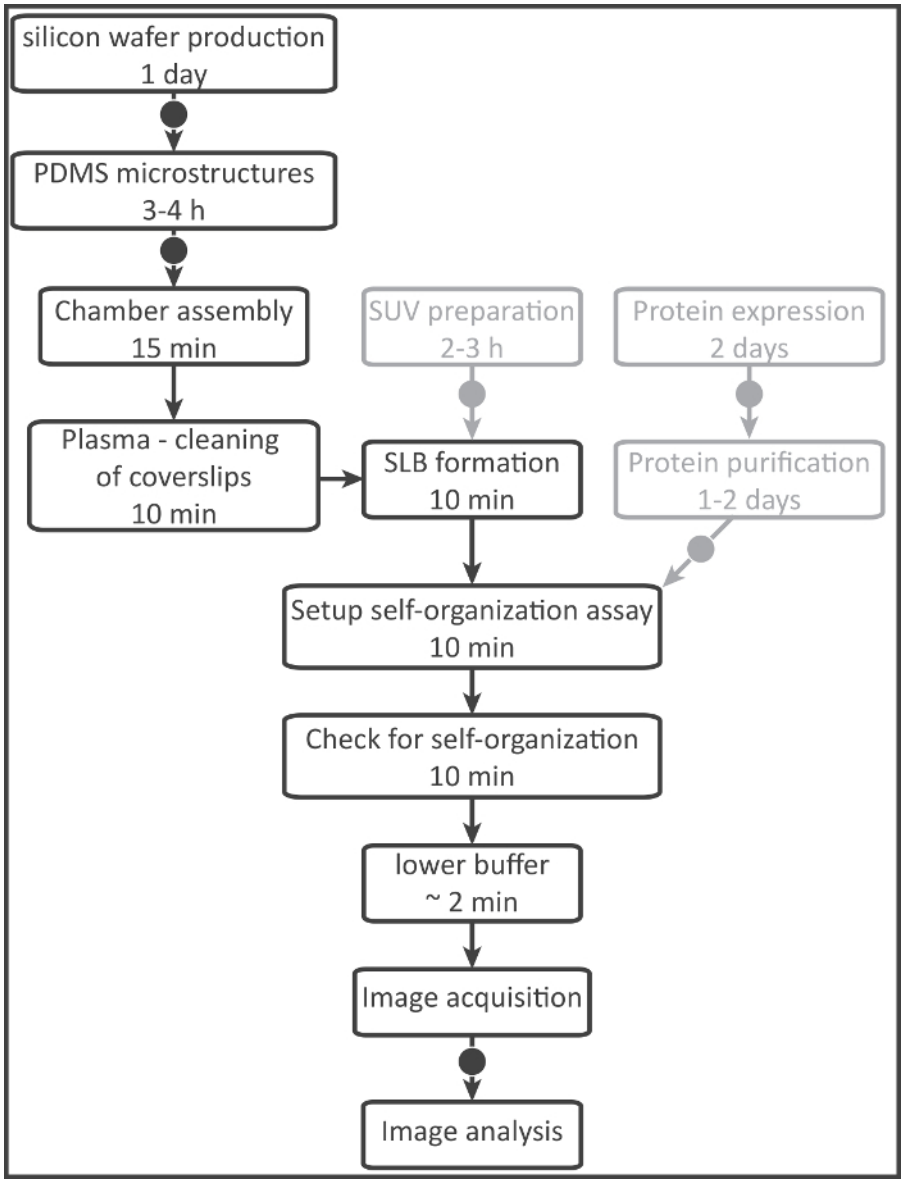

Figure 4: Process flow diagram showing the individual steps and timing of the protocol for self-organization in rod-shaped microstructures (Steps 1-5, 7, 8). Grey boxes indicate steps where products can be reused from the protocol on non-patterned supported lipid bilayers. Arrows marked by circles indicate where the protocol can be paused and resumed later. Please click here to view a larger version of this figure.

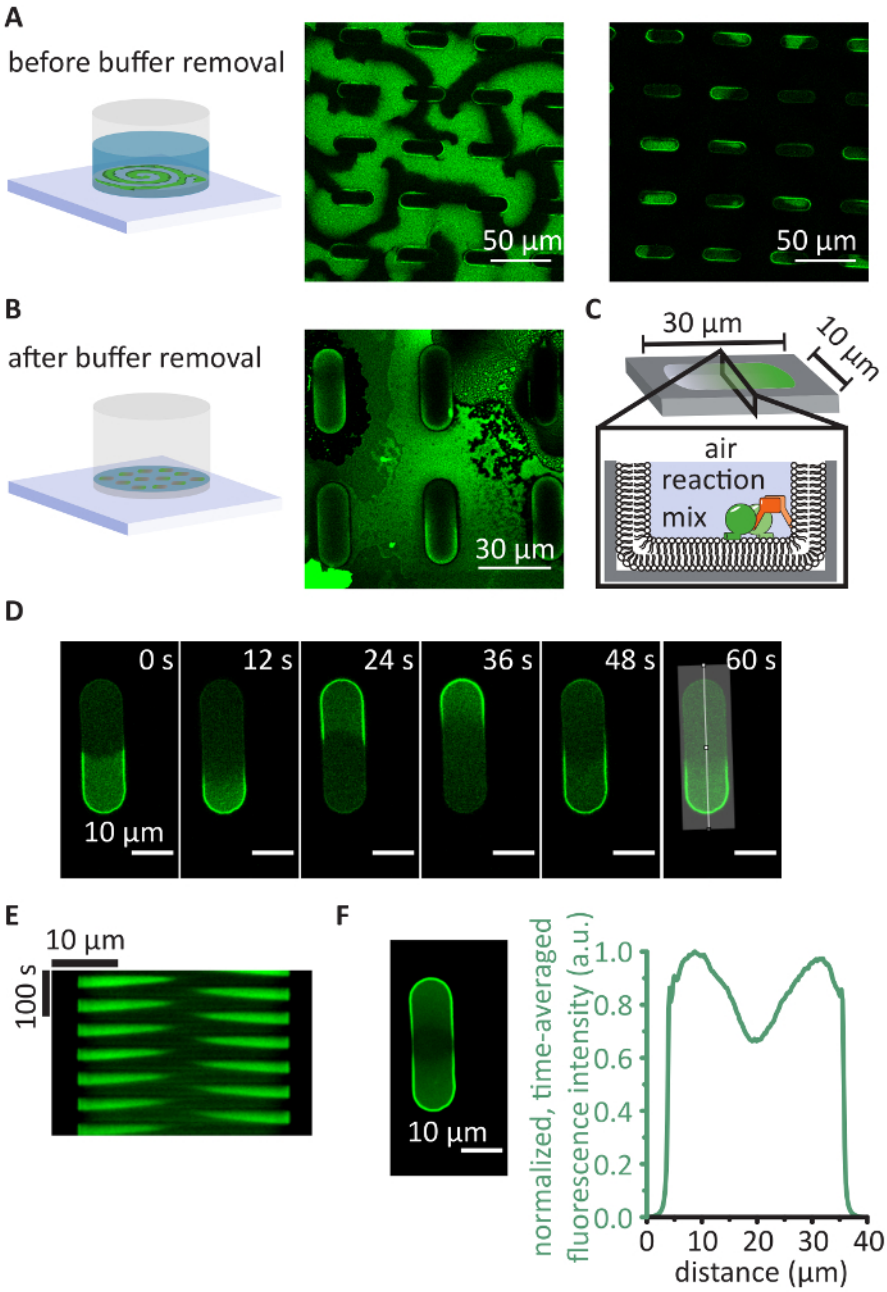

Figure 5: Representative results for MinDE pattern formation in rod-shaped PDMS microcompartments. A) MinDE self-organize on the surface of the PDMS forming traveling surface waves (1 µM MinD (30% EGFP-MinD), 2 µM MinE and 2.5 mM ATP). **B)** After the buffer is lowered to the height of the microstructures, the protein self-organization stops on the planar surface between the microcompartments. **C)** Schematic of one rod-shaped microcompartment. **D)** Representative images of MinDE pole-to-pole oscillations after buffer removal. **E)** Kymograph of the oscillations along the highlighted line shown in D). **F)** Image and profile of the average fluorescence intensity of the time-series shown in D) clearly showing the protein gradient that is maximal at microcompartment poles and minimal at compartment middle. Please click here to view a larger version of this figure.

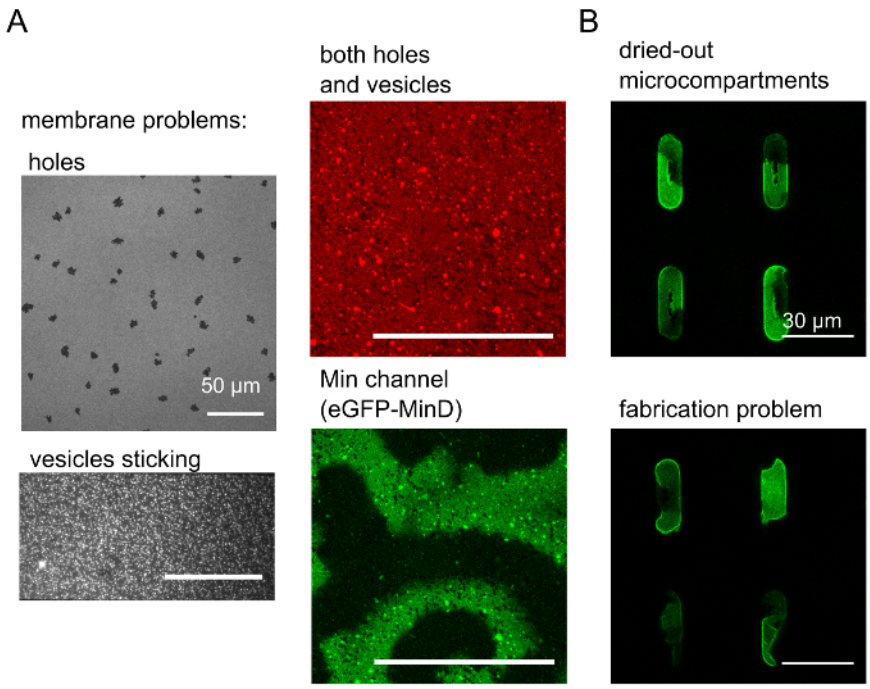

Figure 6: Examples of negative experimental outcomes. A) Over-washed membranes accumulate holes, while suboptimal vesicle preparations and lipid compositions lead to sticking vesicles. The two center panels show a combination of both problems and how they become visible when observing Min oscillations. Membranes were labelled with 0.05% Atto655-DOPE. (scale bars: 50 µm) **B)** Top panel: Dried out microcompartments can be caused by too much buffer removal or when the buffer evaporates over time. Bottom panel: Incomplete compartments can be formed during wafer production or PDMS molding. (scale bars: 30 µm) Please click here to view a larger version of this figure.

Supplementary File 1: Plasmid map for His-MinD. Please click here to download this file.

Supplementary File 2: Plasmid map for His-EGFP-MinD. Please click here to download this file.

Supplementary File 3: Plasmid map for His-mRuby3-MinD. Please click here to download this file.

Supplementary File 4: Plasmid map for His-MinE. Please click here to download this file.

Supplementary File 5: Plasmid map for His-MinC. Please click here to download this file.

Supplementary File 6: CAD file for silicon wafer of rod-shaped microcompartments. Please click here to download this file.

Discussion

We have described a protocol for the *in vitro* reconstitution of MinCDE self-organization on planar supported lipid bilayers and in lipid bilayer covered 3D structures, using the example of rod-shaped PDMS microstructures. In order to obtain valuable data from these assays, the most important factors to control are protein and membrane quality.

To ensure protein quality, protein mass should be confirmed using SDS-PAGE and mass spectrometry. Furthermore, it should be verified that proteins are soluble and not aggregated, by using analytical gel filtration or dynamic light scattering. Gel filtration can be used to remove any aggregated fraction of proteins. Careful pH adjustment and quality of added nucleotides is critical, as the addition of non-adjusted or partially degraded nucleotide to protein stocks or self-organizing assays is sufficient to eliminate protein activity, therefore abolishing self-organization.

Next to protein quality, membrane quality is most critical, and improper membrane formation is most often the cause for defective self-organization and the origin of artefactual surface structures.

When performing the protocol for the first time, it is helpful to label the supported lipid bilayers by including labeled lipids such as Atto-655-DOPE or DiI at low molar percentages (0.05%). Thereby the properties and quality of the membrane can be judged directly. Using FRAP, the fluidity of the membrane can be assessed. Furthermore, one can directly assess the quality of washing of the SLB, as there will either be too many vesicles, no fluid membrane, or no membrane at all, if it has been washed off. The open chamber approach allows to rigorously wash the membrane, and hence also to remove vesicles that are sticking on the surface of the SLB. The most crucial factors for obtaining fluid and homogenous supported lipid bilayers are the cleaning and hydrophilicity of the support surface and the correct size and homogeneity of the SU*Vs.* It can be helpful to check SUV size and size distribution using dynamic light scattering. For narrow size distributions, we recommend

extruding the vesicles rather than sonicating them. Other methods of cleaning coverslips, *e.g.,* treatments with strong bases, basic detergents, or using coverslips directly after rinsing with water, may yield good results, depending on the application and lipid mixture.

The first half of the protocol presented here, *in vitro* reconstitution on planar supported lipid bilayers in open chambers, has the advantage of rendering the surface accessible for optical microscopies, such as TIRF microscopy[30], FRAP analysis[6], single-particle tracking[34], as well as surface probe techniques such as atomic force microscopy[26]. The large homogeneous area allows for better statistics at defined concentrations. Furthermore the open chamber approach allows to precisely control protein concentration and a rapid and simple addition of further components, hence permitting to titrate protein concentration in a single chamber[20]. The assay can also be expanded by addition of other bacterial divisome components such as FtsZ[22,35], ZipA[22] or the chimeric protein FtsZ-YFP-MTS[10,35].

Other groups have taken a similar approach to reconstituting the Min system *in vitro*, but use a flow-cell instead of an open chamber[17,18,19]. Flow-cells have certain advantages, in particular when a fully enclosed 3D environment is needed[18], the influence of flow[17,19,23] or membrane composition[23] on MinCDE patterns is investigated, or if protein patterns are to be observed under protein limiting conditions[19]. Nonetheless, local control of molecular concentrations is more difficult. Protein components, especially MinD, strongly bind to the membrane they first encounter[18,19]. In our experience, the proteins frequently exhibit non-specific binding to tubing, inlets, syringes and other microfluidic parts. Hence, local protein concentrations differ from input concentrations[18] and also vary over the length of the flow-cell, resulting in a variety of different protein patterns on the membrane between inlet and outlet, as observed by others[19].

The second half of the protocol presented here, the *in vitro* reconstitution in rod-shaped microstructures re-using the open chamber approach on a patterned support covered by lipid bilayers allows for a simple mimic of *in vivo* protein behavior even though precise control over protein concentrations is lost due to buffer removal. Note that because the wavelength of MinDE is about one order of magnitude larger *in vitro* than *in vivo* the rod-shaped microcompartments are also about one order of magnitude larger (10 x 30 µm) than a rod-shaped *E. coli* cell.

Overall, this protocol allows for the precise control of all conditions including protein concentration, buffer composition and membrane properties. The use of 3D structured supports enables the reaction to be studied under spatial confinement, mimicking *in vivo* behavior without the need for complex microfluidics equipment.

Disclosures

The authors have nothing to disclose.

Acknowledgements

We thank Michael Heymann and Frank Siedler for production of silicon wafers, Core Facility MPI-B for assistance in protein purification and Simon Kretschmer and Leon Harrington for comments on the manuscript.

References

1. Soh, S., Byrska, M., Kandere-Grzybowska, K., Grzybowski, B.A. Reaction-diffusion systems in intracellular molecular transport and control. *Angew Chemie Int Ed.* **49** (25), 4170-4198 (2010).
2. Lutkenhaus, J. The ParA/MinD family puts things in their place. *Trends Microbiol.* **20** (9), 411-418 (2012).
3. Shih, Y.-L., Zheng, M. Spatial control of the cell division site by the Min system in *Escherichia coli*. *Environ Microbiol.* **15** (12), 3229-3239 (2013).
4. Halatek, J., Frey, E. Highly canalized MinD transfer and MinE sequestration explain the origin of robust MinCDE-protein dynamics. *Cell Rep.* **1** (6), 741-752 (2012).
5. Raskin, D.M., De Boer, P.A.J. MinDE-dependent pole-to-pole oscillation of division inhibitor MinC in *Escherichia coli*. *J Bacteriol.* **181** (20), 6419-6424 (1999).
6. Loose, M., Fischer-Friedrich, E., Ries, J., Kruse, K., Schwille, P. Spatial regulators for bacterial cell division self-organize into surface waves in vitro. *Science.* **320** (5877), 789-792 (2008).
7. Wu, F., van Schie, B.G.C., Keymer, J.E., Dekker, C. Symmetry and scale orient Min protein patterns in shaped bacterial sculptures. *Nat Nanotechnol.* **10** (June), 719-726 (2015).
8. Hu, Z., Lutkenhaus, J. Topological regulation of cell division in E. coli: Spatiotemporal oscillation of MinD requires stimulation of its ATPase by MinE and phospholipid. *Mol Cell.* **7** (6), 1337-1343 (2001).
9. Meinhardt, H., de Boer, P.A.J. Pattern formation in Escherichia coli: A model for the pole-to-pole oscillations of Min proteins and the localization of the division site. *Proc Natl Acad Sci U S A.* **98** (25), 14202-14207 (2001).
10. Zieske, K., Schwille, P. Reconstitution of self-organizing protein gradients as spatial cues in cell-free systems. *Elife.* **3**, e03949 (2014).
11. Roberts, M.A.J., Wadhams, G.H., Hadfield, K.A., Tickner, S., Armitage, J.P. ParA-like protein uses nonspecific chromosomal DNA binding to partition protein complexes. *Proc Natl Acad Sci U S A.* **109** (17), 6698-6703 (2012).
12. Vecchiarelli, A.G., Mizuuchi, K., Funnell, B.E. Surfing biological surfaces: Exploiting the nucleoid for partition and transport in bacteria. *Mol Microbiol.* **86** (3), 513-523 (2012).
13. Thanbichler, M., Shapiro, L. MipZ, a spatial regulator coordinating chromosome segregation with cell division in Caulobacter. *Cell.* **126** (1), 147-162 (2006).
14. Lim, H.C., Surovtsev, I.V., Beltran, B.G., Huang, F., Bewersdorf, J., Jacobs-Wagner, C. Evidence for a DNA-relay mechanism in ParABS-mediated chromosome segregation. *Elife.* **3**, e02758 (2014).
15. Mileykovskaya, E., Fishov, I., Fu, X., Corbin, B.D., Margolin, W., Dowhan, W. Effects of phospholipid composition on MinD-membrane interactions *in vitro* and *in vivo*. *J Biol Chem.* **278** (25), 22193-22198 (2003).
16. Renner, L.D., Weibel, D.B. Cardiolipin microdomains localize to negatively curved regions of Escherichia coli membranes. *Proc Natl Acad Sci U S A.* **108** (15), 6264-6269 (2011).

17. Ivanov, V., Mizuuchi, K. Multiple modes of interconverting dynamic pattern formation by bacterial cell division proteins. *Proc Natl Acad Sci U S A.* **107** (18), 8071-8078 (2010).
18. Caspi, Y., Dekker, C. Mapping out Min protein patterns in fully confined fluidic chambers. *Elife.* **5**, e19271 (2016).
19. Vecchiarelli, A.G. *et al.* Membrane-bound MinDE complex acts as a toggle switch that drives Min oscillation coupled to cytoplasmic depletion of MinD. *Proc Natl Acad Sci U S A.* **113** (11), E1479-E1488 (2016).
20. Kretschmer, S., Zieske, K., Schwille, P. Large-scale modulation of reconstituted Min protein patterns and gradients by defined mutations in MinE's membrane targeting sequence. *PLoS One.* **12** (6), e0179582 (2017).
21. Schweizer, J., Loose, M., Bonny, M., Kruse, K., Monch, I., Schwille, P. Geometry sensing by self-organized protein patterns. *Proc Natl Acad Sci.* **109** (38), 15283-15288 (2012).
22. Martos, A., Raso, A., Jiménez, M., Petrášek, Z., Rivas, G., Schwille, P. FtsZ polymers tethered to the membrane by ZipA are susceptible to spatial regulation by min waves. *Biophys J.* **108** (9), 2371-2383 (2015).
23. Vecchiarelli, A.G., Li, M., Mizuuchi, M., Mizuuchi, K. Differential affinities of MinD and MinE to anionic phospholipid influence Min patterning dynamics *in vitro*. *Mol Microbiol.* **93** (3), 453-463 (2014).
24. Glock, P. *et al.* Optical control of a biological reaction-diffusion system. *Angew Chemie Int Ed.* **57** (9), 2362-2366 (2018).
25. Zieske, K., Schwille, P. Reconstitution of pole-to-pole oscillations of min proteins in microengineered polydimethylsiloxane compartments. *Angew Chemie Int Ed.* **52** (1), 459-462 (2013).
26. Miyagi, A., Ramm, B., Schwille, P., Scheuring, S. High-speed AFM reveals the inner workings of the MinDE protein oscillator. *Nano Lett.* **18** (1), 288-296 (2017).
27. Ramirez-Diaz, D.A. et al. Treadmilling analysis reveals new insights into dynamic FtsZ ring architecture. *PLoS Biol.* **16** (5), e2004845 (2018).
28. Vogel, S.K., Petrasek, Z., Heinemann, F., Schwille, P. Myosin motors fragment and compact membrane-bound actin filaments. *Elife.* **2**, e00116 (2013).
29. Zieske, K., Schweizer, J., Schwille, P. Surface topology assisted alignment of Min protein waves. *FEBS Lett.* **588** (15), 2545-2549 (2014).
30. Loose, M., Fischer-Friedrich, E., Herold, C., Kruse, K., Schwille, P. Min protein patterns emerge from rapid rebinding and membrane interaction of MinE. *Nat Struct Mol Biol.* **18** (5), 577-583 (2011).
31. Zieske, K., Schwille, P. Reconstituting geometry-modulated protein patterns in membrane compartments. *Methods Cell Biol.* **128**, 149-163 (2015).
32. Gruenberger, A., Probst, C., Heyer, A., Wiechert, W., Frunzke, J., Kohlheyer, D. Microfluidic picoliter bioreactor for microbial single-cell analysis: fabrication, system setup, and operation. *J Vis Exp.* (82), e50560 (2013).
33. Schindelin, J. *et al.* Fiji: An open-source platform for biological-image analysis. *Nat Methods.* **9** (7), 676-682 (2012).
34. Loose, M., Kruse, K., Schwille, P. Protein self-organization: Lessons from the min system. *Annu Rev Biophys.* **40**, 315-336 (2011).
35. Arumugam, S., Petrašek, Z., Schwille, P. MinCDE exploits the dynamic nature of FtsZ filaments for its spatial regulation. *Proc Natl Acad Sci U S A.* **111** (13), E1192-E1200 (2014).